



# Synergistic effects of Pd decoration and substrates on the NO<sub>2</sub> sensing performance of sprayed WO<sub>3</sub> thin films

Vinayak Ganbavle<sup>a</sup>, Shahin Shaikh<sup>b</sup>, Santosh Mohite<sup>c</sup>, Sumayya Inamdar<sup>d</sup>, Amit Bagade<sup>e</sup>, Atish Patil<sup>a</sup>, Keshav Rajpure<sup>f,\*</sup>

<sup>a</sup> Dattajirao Kadam Arts, Science and Commerce College, Ichalkaranji 416115, M.S., India

<sup>b</sup> Karmveer Bhaurao Patil College of Engineering, Satara 415001, M.S., India

<sup>c</sup> Department of Applied Chemistry, Konkuk University, Chungju 27478, Republic of Korea

<sup>d</sup> Vivekanand College of Kolhapur, 416003 M.S., India

<sup>e</sup> Sharad Institute of Technology, Engineering, Yadav, Ichalkaranji 416121, M.S., India

<sup>f</sup> Electrochemical Materials Laboratory, Department of Physics, Shivaji University, Kolhapur, M.S., India

## ARTICLE INFO

### Keywords:

NO<sub>2</sub> sensor  
Selectivity  
WO<sub>3</sub> thin films  
Pd decoration  
Alumina substrate

## ABSTRACT

The selective detection of NO<sub>2</sub> is achieved using Pd decorated WO<sub>3</sub> thin films deposited on glass (WO<sub>3</sub><sup>G</sup>) and alumina (WO<sub>3</sub><sup>A</sup>) substrates. WO<sub>3</sub><sup>A</sup> film shows superior performance over WO<sub>3</sub><sup>G</sup> film in terms of sensitivity, response magnitude and response and recovery time. Lower detection limit of 2 ppm is achieved using WO<sub>3</sub><sup>A</sup> film for which gas response was 20 % whereas for WO<sub>3</sub><sup>G</sup> film response was 9 %. In particular, higher gas response towards NO<sub>2</sub> is observed for WO<sub>3</sub><sup>A</sup> film, which is attributed to the high surface roughness and high catalytic activity of Pd causing enhanced spillover and effective diffusion of NO<sub>2</sub>.

## 1. Introduction

The higher value of response and selectivity of WO<sub>3</sub> thin film sensor towards NO<sub>2</sub> in comparison with the other metal oxide semiconductors (MOS) makes it more suitable MOS for detection of NO<sub>2</sub> [1]. Taking into account the potential of WO<sub>3</sub> thin films in the field of NO<sub>2</sub> sensor, it is worth making an attempt to lower the lower detection limit and increase the gas response. Thus, in recent years, many of the efforts have been directed at achieving high selectivity, and sensitivity. Efforts made include addition of noble metals or oxide catalysts, manipulation of the sensor temperature and compositional control of sensor. Amongst all these efforts noble metals are effective oxidation catalysts and this property can be used to increase the rate of reaction of the analyte gas with the sensor surface and thereby sensor response is improved [2]. Significant sensor properties such as selectivity, response magnitude and response kinetics can be improved by decorating surface of MOS with the noble metals such as palladium (Pd), platinum (Pt), gold (Au) and silver (Ag) [3–6]. In the fabrication of commercial gas sensors, a low concentration dispersion of metal additives has been practiced over a long time but the working principle of such noble metal decorated MOS is still not entirely understood [7]. To enhance the gas response

properties various noble metals were used like Pd, Pt, Au and Ag. Among all these Pd is the most often used catalyst due to its popular catalytic properties and low cost as compared with Pt and Au. Various methods such as sol–gel, impregnation, thermal evaporation, and sputtering have been used for decorating the surface of the sensor with noble metal additives [8]. Patil et al. [9] reported morphological and crystal structural dependent NO<sub>2</sub> gas sensing properties of WO<sub>3</sub> films prepared using NaOH as an etching agent by hydrothermal method at 100°C and shown that button rose WO<sub>3</sub> sensor is highly sensitive towards NO<sub>2</sub>. Younes et al. demonstrated enhancement in sensing performance towards CO<sub>2</sub> and LPG using Pd decorated WO<sub>3</sub> nano particles. They have shown improvement in CO<sub>2</sub> and LPG sensing by incorporating palladium by varying doping level [10]. Various reports show that Pd decoration not only improves gas response selectively towards target gas but also reduces response kinetics and sometimes operating temperature of the sensor [2]. Along with this it has also been studied that surface roughness of the substrates also plays important role in gas sensing performance of the films. Thus along with glass films are deposited on alumina substrates simultaneously and were used for the fabrication of sensor.

In this paper, we discuss the enhancement in the NO<sub>2</sub> sensing properties of the WO<sub>3</sub> thin film sensor deposited using spray pyrolysis

\* Corresponding author.

E-mail address: [shahin.savalaj@gmail.com](mailto:shahin.savalaj@gmail.com) (K. Rajpure).

<https://doi.org/10.1016/j.cplett.2023.140327>

Received 22 July 2022; Received in revised form 18 January 2023; Accepted 18 January 2023

Available online 21 January 2023

0009-2614/© 2023 Published by Elsevier B.V.

technique on alumina and glass substrates and Pd decoration is carried via a simple chemical method.

## 2. Experimental procedure

WO<sub>3</sub> films were deposited on alumina and glass substrates (purchased from Blue Star India) by spray pyrolysis technique using peroxotungstic acid (PTA). PTA is commercially purchased from Labtronics India Pvt. Ltd. and it is used without further purification. The optimized deposition parameters were 425 °C substrate temperature, 15 mM solution concentration, 100 ml solution quantity, 28 cm nozzle to substrate distance and 5 ml/min spray rate [11]. These films were then decorated with Pd using palladium chloride (PdCl<sub>2</sub>) (s. d. fine chem. limited, Mumbai) using dip coating. The films were dipped in 10 mM PdCl<sub>2</sub> solution for 10 min, dried at room temperature and then heat treated for 2 h at 200 °C to remove chlorine from the deposit [12]. Five such cycles were carried out in order to disperse Pd uniformly in the film surface. These Pd decorated WO<sub>3</sub> thin films were then used for further characterization and gas sensing measurements. The Pd decorated WO<sub>3</sub> film deposited on glass substrate was labeled as WO<sub>3</sub><sup>G</sup> and that on alumina substrate was labeled as WO<sub>3</sub><sup>A</sup>.

Surface morphology and topography were studied using scanning electron microscopy (SEM) and atomic force microscopy (AFM). To verify the dispersion of the Pd in the surface, the energy dispersive X-ray analysis (EDX) was carried out. To examine the effect of the decoration on the gas sensing properties, the films were subjected to gas sensing measurements with respect to temperature and gas concentration. Gas sensing measurements were carried out in a locally fabricated gas sensing unit equipped with temperature controller and Keithley electrometer-6514. Film of size 1 cm × 1 cm was used as a sensor and canisters of 2000 ppm gas concentration (Shreya Enterprises, Mumbai) were used to prepare gas of desired concentration.

## 3. Results and discussion

### 3.1. Scanning electron microscopy

Fig. 1 (a) and (b) show SEM images of morphology of WO<sub>3</sub><sup>A</sup> and WO<sub>3</sub><sup>G</sup> films which are distinct for both the films. Fibrous reticulated network is observed for WO<sub>3</sub><sup>G</sup> whereas spherical grains are observed for WO<sub>3</sub><sup>A</sup>. This difference is due to the different surface roughness and different number of nucleation centers available on the substrates surface. It is clearly observed that the WO<sub>3</sub><sup>G</sup> film is porous than the WO<sub>3</sub><sup>A</sup> film and thus conduction channel may be available within the grains for WO<sub>3</sub><sup>A</sup> film. AFM measurement was carried out (not shown) to measure surface roughness of the films. It is revealed from the AFM studies that WO<sub>3</sub><sup>A</sup> possesses higher surface roughness (170 nm) than WO<sub>3</sub><sup>G</sup> (83 nm) film. This is due to the higher roughness of alumina substrate than the glass substrate. Since more analyte gas molecules can be adsorbed on the film with high

surface roughness, WO<sub>3</sub><sup>A</sup> exhibited higher gas response than WO<sub>3</sub><sup>G</sup>. Further voids formed in between the grains for WO<sub>3</sub><sup>A</sup> film provide more effective surface area and effective distribution of catalyst enhances gas response of the films.

### 3.2. Energy dispersive X-ray analysis

The EDX spectra of WO<sub>3</sub><sup>A</sup> and WO<sub>3</sub><sup>G</sup> films are shown in Fig. 2 (a) and (b). In both the patterns, prominent peaks corresponding to emission of characteristic X-rays by W, O and Pd are clearly visible. This confirms the dispersion of Pd in the film surface. Absence of any other peaks except those due to Pd, W and O in both spectra indicates the formation of films without any elemental impurities. The area under the curve of the EDX is used for the quantification of the composition of elements present in the film surface. The compositional values of atomic and weight percentage for W, O and Pd are mentioned in Table 1. Pd in WO<sub>3</sub><sup>G</sup> film surface is 0.24 at % and that in WO<sub>3</sub><sup>A</sup> film surface is 0.42 at %. This ensures the existence of Pd catalyst in the surface of the films. The O/W ratio observed for WO<sub>3</sub><sup>A</sup> and WO<sub>3</sub><sup>G</sup> films is 3.53 and 3.10, respectively. Higher oxygen content than the stoichiometric WO<sub>3</sub> can be attributed to the adsorbed oxygen and water in the surface [13].

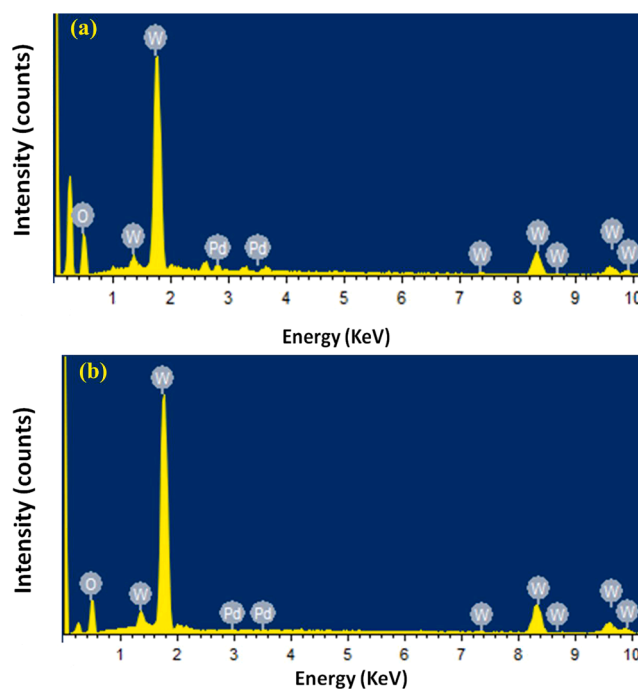


Fig. 2. EDX spectra of (a) WO<sub>3</sub><sup>A</sup> (b) WO<sub>3</sub><sup>G</sup> films.

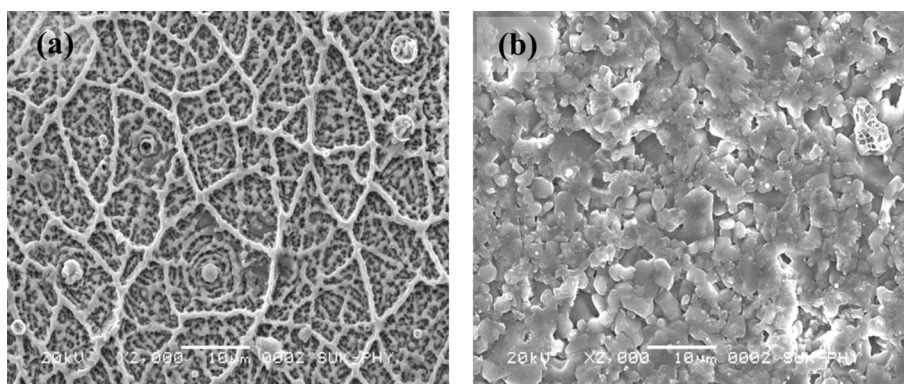


Fig. 1. SEM images of Pd decorated WO<sub>3</sub> films deposited on (a) alumina (WO<sub>3</sub><sup>A</sup>) and (b) glass (WO<sub>3</sub><sup>G</sup>) substrates.

**Table 1**  
Percentage compositions of  $\text{WO}_3^{\text{A}}$  and  $\text{WO}_3^{\text{G}}$  films measured using EDX spectra.

Element	$\text{WO}_3^{\text{A}}$		$\text{WO}_3^{\text{G}}$	
	Weight %	Atomic %	Weight %	Atomic %
O K	21.08	75.29	23.40	77.75
Pd L	0.77	0.42	0.47	0.24
W M	78.15	24.29	76.13	22.01
Total	100.00	100.00	100.00	100.00

### 3.3. Gas sensing properties

Gas sensing measurements of Pd sensitized  $\text{WO}_3$  thin films were carried out at different operating temperatures and towards various  $\text{NO}_2$  concentrations. Gas response of the sensor was calculated using the formula:

$$S = \left[ \frac{R_g - R_a}{R_a} \right] \times 100 \quad (1)$$

Where  $R_g$  is the resistance of the sensor in presence of analyte gas and  $R_a$  is the resistance of the sensor in presence of air. The response time is measured as the time taken by sensor to reach 90 % of its maximum gas response in the presence of analyte gas and recovery time is the time taken by the sensor to reach 10 % of the maximum gas response upon removal of analyte gas. As the operating temperature plays an important role in deciding the sensor performance, it was optimized by measuring gas response at various temperatures.

#### 3.3.1. Determination of operating temperature

The optimum operating temperature was determined by measuring the gas response when both,  $\text{WO}_3^{\text{G}}$  and  $\text{WO}_3^{\text{A}}$  films were exposed to 100 ppm  $\text{NO}_2$  over the temperature range of 50 to 250 °C as shown in Fig. 3. Surface modification was expected to enhance the gas response, improve the response, recovery time and reduce the optimal operating temperature of the sensor. [14] Increase in gas response was observed with operating temperature and the maximum response of 134 and 192 % were observed for  $\text{WO}_3^{\text{G}}$  and  $\text{WO}_3^{\text{A}}$  films, respectively at 200 °C towards 100 ppm  $\text{NO}_2$ . Gas response decreased at operating temperature higher than 200 °C due to higher rate of desorption of  $\text{NO}_2$  than that of adsorption and dissociation of  $\text{NO}_2$  molecules before adsorption on the sensor surface. Increase in the gas response by an amount of 24.4 and

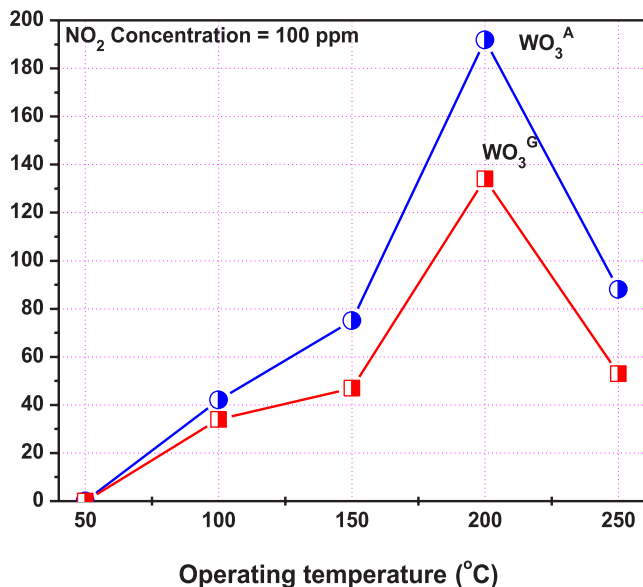
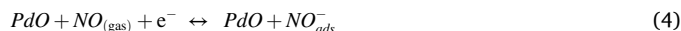


**Fig. 3.** Variation in gas response of  $\text{WO}_3^{\text{A}}$  and  $\text{WO}_3^{\text{G}}$  towards 100 ppm  $\text{NO}_2$  at different operating temperatures.

37.7 % in comparison with pristine films was observed for Pd decorated films on glass and alumina substrates, respectively (not shown). High rate of spillover and dissociation of the  $\text{NO}_2$  at Pd modified sites enhanced the kinetics of the reactions and improved the gas response thus decreased the response and recovery time [15]. Moreover more uniform distribution of Pd in the surface of film deposited on alumina substrates enhances gas response of  $\text{WO}_3^{\text{A}}$  film. It is observed that Pd decorated  $\text{WO}_3$  films show improved gas response and sensor kinetics whereas operating temperature of the sensor remains same as those for pristine films. The transient response curves  $\text{WO}_3^{\text{G}}$  and  $\text{WO}_3^{\text{A}}$  films are presented in Figs. 4 and 5. At lower operating temperature (50 °C) both the sensors do not respond to  $\text{NO}_2$  due to the insufficient thermal energy for the reaction and charge transfer. At 100 °C operating temperature,  $\text{WO}_3^{\text{G}}$  film showed irreversible gas response (Fig. 4) while  $\text{WO}_3^{\text{A}}$  film shows reversible response of magnitude 42 % (Fig. 5). At 100 °C, the resistance of the sensor could not regain its original value even after 1 h for  $\text{WO}_3^{\text{G}}$  film resulting in irreversible gas response. Both the films showed higher gas response after decoration with Pd and the similar results are reported by Karpe et. al. [16]. At 200 °C, the response was seen to be highest for both  $\text{WO}_3^{\text{G}}$  and  $\text{WO}_3^{\text{A}}$  films. Response and recovery time corresponding to different measurements are tabularized in Table 2. Both Pd decorated films show improved response kinetics as compared with the pristine  $\text{WO}_3$  films. Fast response and recovery was observed because of the spillover effect due to the presence of Pd in the films surface. As expected the response and recovery time decreased with increase in operating temperature.

#### 3.3.2. $\text{NO}_2$ sensing mechanism

In general for MOS, gas sensing mechanism involves change in surface resistance due to the chemisorption of oxygen molecules. These oxygen species adsorbed on the surface by capturing the free electron from metal oxide [17]. The chemisorption of oxygen molecules depends upon the operating temperature of the sensor and with respect to operating temperature absorbed  $\text{O}_2$  molecule convert to oxygen ions (e. g.  $\text{O}_2^-$ ,  $\text{O}^-$  or  $\text{O}^{2-}$ ) [18]. Effective catalytic dissociation ability of noble metals especially Pd makes it popular for the surface modification to enhance the gas sensing properties of the MOS sensors. There are, in general, two schemes of the gas sensing mechanism when the effect of additive is to be considered. The reaction of analyte gas occurs at the oxide surface and the role of the additive metal particles is to increase the metal oxide surface coverage in order to increase the active surface area for adsorption of gas molecules. The introduction of additives generates new adsorption sites. These particles are involved in the adsorption reaction and the metal oxide has a function of transducing the electrochemical changes into change in resistance of the sensor. Reactions involved in  $\text{NO}_2$  sensing due to Pd decoration are given below [19]:



It is supposed that the reduction/oxidation of analyte gas is initiated by the metal additives by forming the active surface species. When analyte gas comes in contact with the Pd, due to its catalytic activity, the gas gets dissociated easily and chemisorbed on the sensor surface [2]. The adsorption reaction is enhanced by the spillover process and large number of gas molecules at higher rate is adsorbed at the surface of the sensor. The transducer function which corresponds to the ability to convert the signal caused by chemical interaction of the oxide surface into electrical signal is effectively improved by addition of the catalyst on the surface of the sensor as shown in Fig. 6. It is believed that the adsorbed gas molecules reside on oxide support and diffuse into the host MOS through Pd particle on the surface before it has had an opportunity to desorb [15]. An effective reaction zone is formed at the catalyst sites

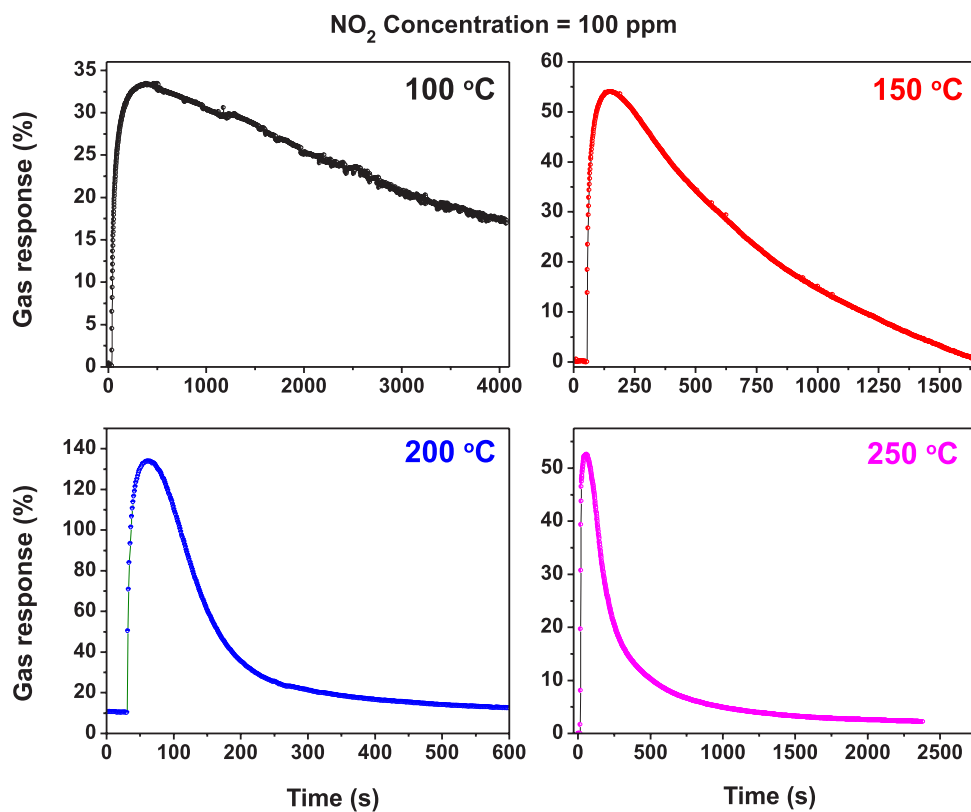


Fig. 4. Transient gas response curves of WO<sub>3</sub><sup>G</sup> film towards 100 ppm NO<sub>2</sub> at different operating temperatures.

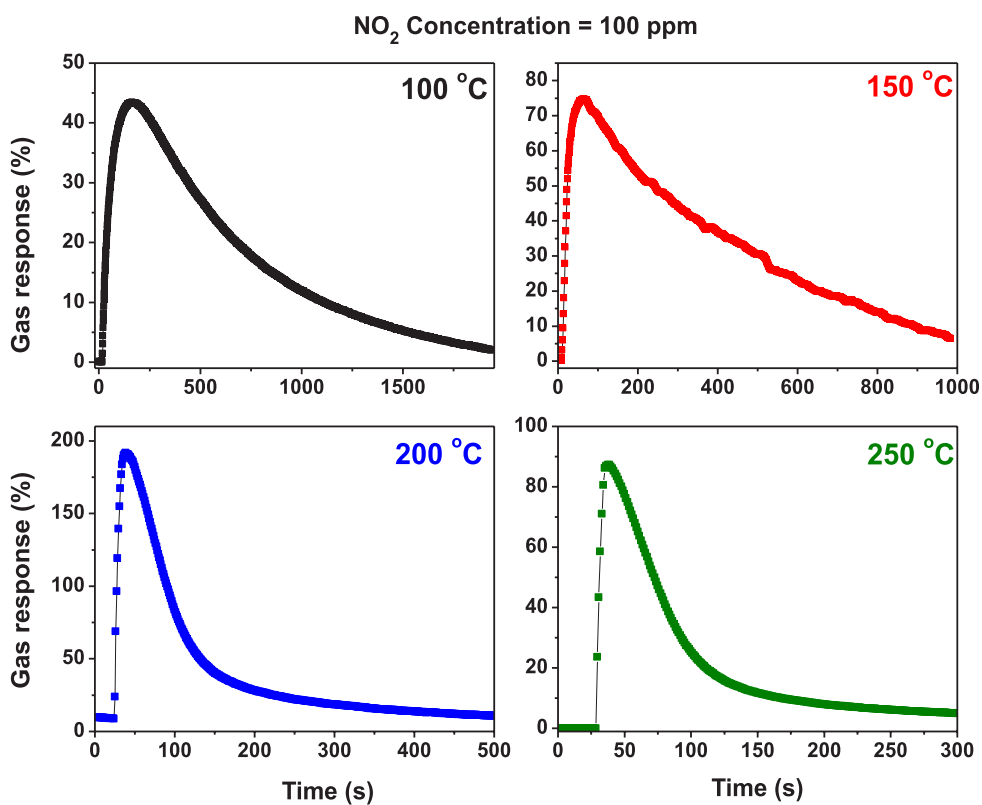


Fig. 5. Transient gas response curves of WO<sub>3</sub><sup>A</sup> film towards 100 ppm NO<sub>2</sub> at different operating temperatures.



**Table 2**

Response and recovery time of  $\text{WO}_3^{\text{A}}$  and  $\text{WO}_3^{\text{G}}$  films towards 100 ppm  $\text{NO}_2$  at different operating temperatures.

Operating temperature ( $^{\circ}\text{C}$ )	$\text{WO}_3^{\text{A}}$		$\text{WO}_3^{\text{G}}$	
	Response time (s)	Recovery time (s)	Response time (s)	Recovery time (s)
100	83	1396	114	>3000
150	19	889	34	1190
200	11	292	13	457
250	4	53	9	830

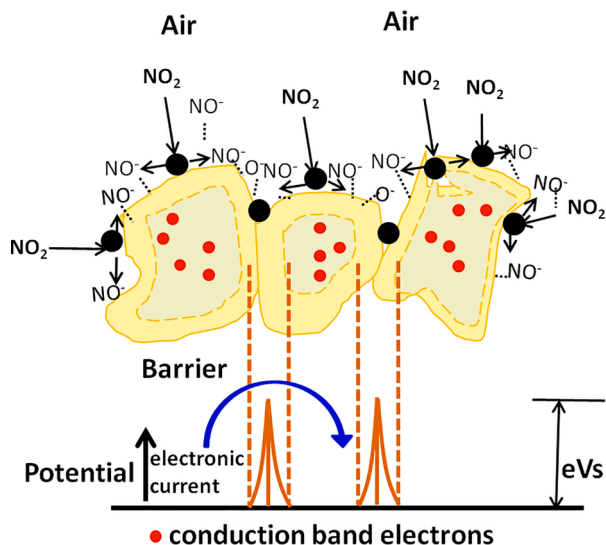


Fig. 6. Schematic of gas sensing mechanism on Pd decorated MOS surface.

as compared with that at pristine sites and whole surface of metal oxide near to the catalyst gets covered by the adsorbed oxygen and  $\text{NO}_2$ . Thus, it is important to ensure the uniform dispersion of catalysts in to the sensor surface so that the adsorption accelerated on the surface decorated with the Pd than that on the pristine MOS surface.

### 3.3.3. Effect of $\text{NO}_2$ concentration and selectivity studies

Concentration dependent gas sensing studies for both the films were carried out at the optimum operating temperature. Enhanced gas response of the sensor at the optimal operating temperature encouraged to test the sensor at lower concentrations of  $\text{NO}_2$ . As expected, with increase in the  $\text{NO}_2$  concentration from 2 ppm to 100 ppm, the gas response increases at faster rate initially and then gradually at higher concentration, both types of films. Figs. 7 and 8 show variation in gas response with respect to  $\text{NO}_2$  concentration for  $\text{WO}_3^{\text{G}}$  and  $\text{WO}_3^{\text{A}}$  films, respectively. Figures show 9 and 20 % gas response for  $\text{WO}_3^{\text{G}}$  and  $\text{WO}_3^{\text{A}}$  films, respectively towards 2 ppm  $\text{NO}_2$  operating at 200  $^{\circ}\text{C}$ . This concentration of  $\text{NO}_2$  is 10 times lower than the immediately dangerous to life or health (IDLH) concentration [20] and is less than half of the short term exposure limit (5 ppm) for  $\text{NO}_2$ . When pristine sensor was exposed to lower concentration (2 ppm) of  $\text{NO}_2$ , the gas either dissociates in the air itself before reaching the sensor surface or if it is adsorbed on the sensor surface, the change is very small to detect and sensor could not sense the gas at lower concentrations. Conversely, when sensor surface is decorated with Pd, spillover and fast diffusion of  $\text{NO}_2$  at the surface makes it easy to detect  $\text{NO}_2$  even at lower concentration. Thus, Pd decoration enhances the rate of reaction thereby decreasing response and recovery time and it also enables the sensor to detect the lower concentrations. Considerable increase in sensitivity of the sensor is observed after decorating the surface with Pd. At lower concentration range of 2–10 ppm of  $\text{NO}_2$ , the sensitivity is as high as 3.8 %/ppm for

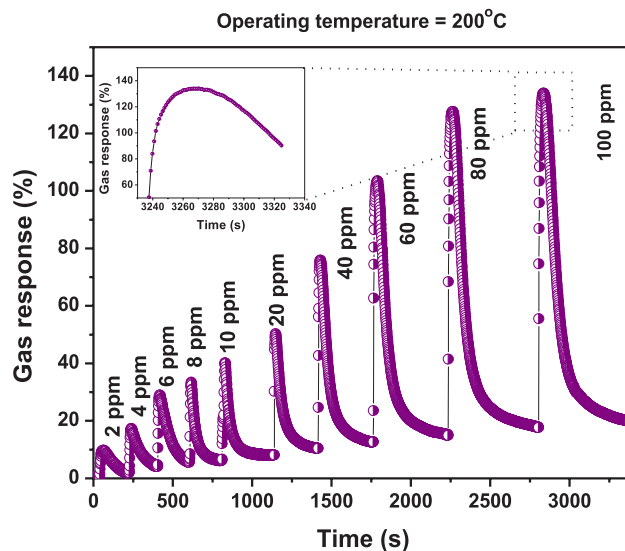


Fig. 7. Transient gas response curve of  $\text{WO}_3^{\text{G}}$  film towards various  $\text{NO}_2$  concentrations at 200  $^{\circ}\text{C}$  operating temperature. Inset shows enlarged view of selected area.

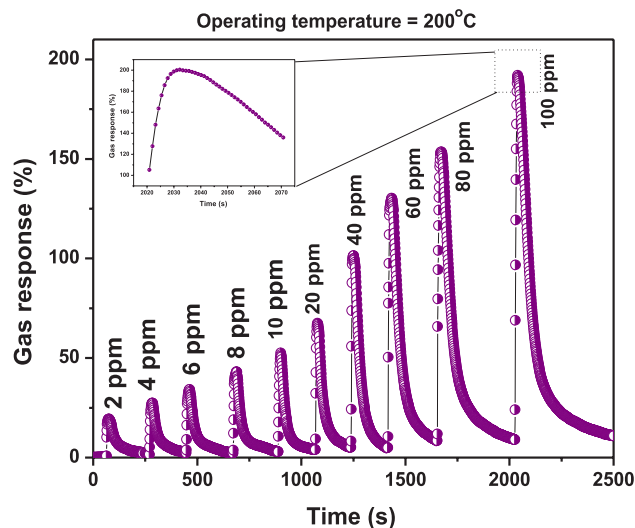


Fig. 8. Transient gas response curve of  $\text{WO}_3^{\text{A}}$  film towards various  $\text{NO}_2$  concentrations at 200  $^{\circ}\text{C}$  operating temperature. Inset shows enlarged view of selected area.

$\text{WO}_3^{\text{G}}$  film and 4.2 %/ppm for  $\text{WO}_3^{\text{A}}$  film. At higher concentrations the response saturates and remains nearly constant as shown in Fig. 9. The results indicate that at lower gas concentrations, gas response is concentration dependent unlike that for higher concentration. Higher gas sensitivity is the key factor deciding detection lower gas concentrations as recognized by international standards. Response and recovery time of  $\text{WO}_3^{\text{A}}$  and  $\text{WO}_3^{\text{G}}$  films towards various  $\text{NO}_2$  concentrations are shown in Table 3. Response and recovery time increased linearly with increase in  $\text{NO}_2$  concentration due to the corresponding increase in the gas response. It takes larger time to cause large change in resistance value thus response and recovery time increases with increase in  $\text{NO}_2$  concentration. To test the selectivity, the sensor was exposed to various gases and response towards each gas was recorded. Fig. 10 shows bar graph of gas versus gas response indicating that the films are highly selective towards  $\text{NO}_2$ . When  $\text{WO}_3^{\text{G}}$  and  $\text{WO}_3^{\text{A}}$  were exposed to various gases viz.  $\text{H}_2\text{S}$ ,  $\text{NH}_3$ , LPG, CO,  $\text{SO}_2$  and  $\text{NO}_2$  of equal concentration at optimized operating temperature of 200  $^{\circ}\text{C}$ , exceptionally high response

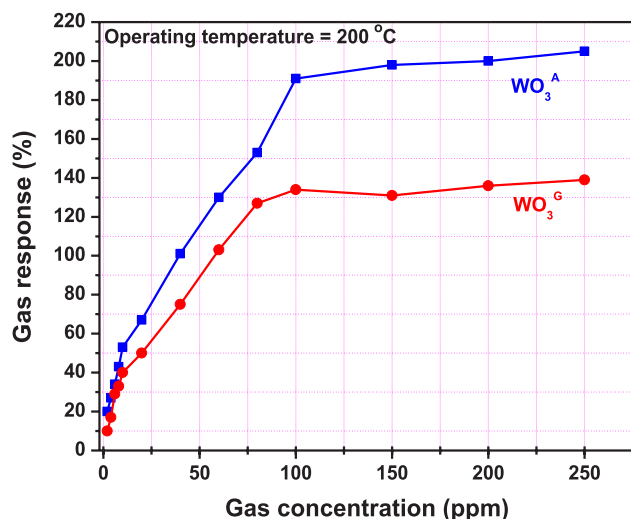


Fig. 9. Variation in gas response with NO<sub>2</sub> concentration of WO<sub>3</sub><sup>G</sup> and WO<sub>3</sub><sup>A</sup> operated at 200 °C.

Table 3

Response and recovery time of WO<sub>3</sub><sup>A</sup> and WO<sub>3</sub><sup>G</sup> films towards various NO<sub>2</sub> concentrations operated at 200 °C.

Gas concentration (ppm)	WO <sub>3</sub> <sup>G</sup>		WO <sub>3</sub> <sup>A</sup>	
	Response time (s)	Recovery time (s)	Response time (s)	Recovery time (s)
2	6	138	4	70
4	7	164	5	85
6	7	166	5	89
8	8	169	5	86
10	8	179	5	89
20	8	184	5	98
40	9	201	6	128
60	9	277	9	141
80	10	380	11	214
100	13	457	13	292

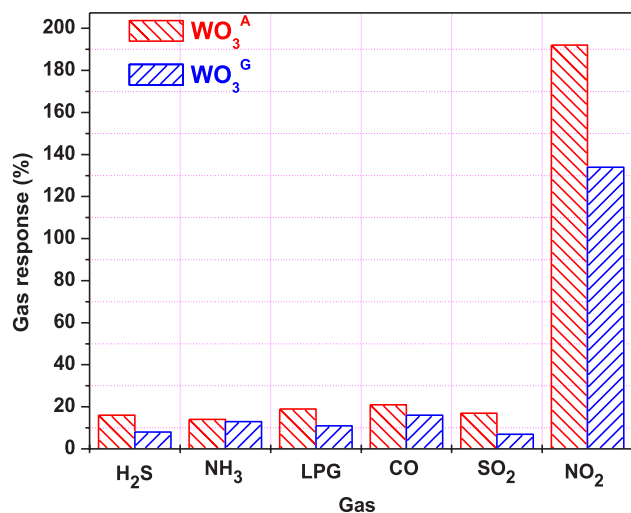


Fig. 10. Selectivity study of WO<sub>3</sub><sup>G</sup> and WO<sub>3</sub><sup>A</sup> towards various gases of 100 ppm concentration at 200 °C operating temperature.

Table 4

Selectivity coefficient of WO<sub>3</sub><sup>G</sup> and WO<sub>3</sub><sup>A</sup> towards various gases.

Gas	Selectivity coefficient	
	WO <sub>3</sub> <sup>G</sup>	WO <sub>3</sub> <sup>A</sup>
H <sub>2</sub> S	17	12
NH <sub>3</sub>	10	14
LPG	12	10
CO	8	9
SO <sub>2</sub>	19	11

was observed for NO<sub>2</sub>. This was indication that the films were still selective towards NO<sub>2</sub> after Pd decoration. The selectivity coefficient [21] of WO<sub>3</sub><sup>A</sup> is lower as compared to WO<sub>3</sub><sup>G</sup> which indicates that WO<sub>3</sub><sup>G</sup> films were more selective towards NO<sub>2</sub>. Selectivity coefficient of the WO<sub>3</sub><sup>G</sup> and WO<sub>3</sub><sup>A</sup> films are mentioned in Table 4.

#### 4. Summary and conclusions

In summary, it is observed that Pd decoration not only enhances the gas response, reduces response and recovery time but also lowers the lower detection limit to a remarkable value. Different substrates can be used to monitor surface morphology and thus gas sensing performance of the sensors. Presence of Pd in the surface of the films was confirmed by the EDX studies. Enhanced gas response of 134 % and 192 % was recorded due to Pd decoration and the corresponding response and recovery time were 13 s, 457 s and 13 s, 292 s for WO<sub>3</sub><sup>G</sup> and WO<sub>3</sub><sup>A</sup> films, respectively. Sensor fabricated on alumina substrate showed appreciable gas response towards 2 ppm of NO<sub>2</sub> which is 10 times lower concentration than IDLH concentration and short term exposure limit of NO<sub>2</sub>. Sensitivity of the sensor was as high as 4.2 %/ppm and 3.8 %/ppm for WO<sub>3</sub><sup>A</sup> and WO<sub>3</sub><sup>G</sup> films, respectively. Along with the gas response and response kinetics, the selectivity of the sensor is high towards NO<sub>2</sub>.

#### Declaration of Competing Interest

The authors declare that they have no known competing financial interests or personal relationships that could have appeared to influence the work reported in this paper.

#### Data availability

The data that has been used is confidential.

#### Appendix A. Supplementary material

Supplementary data to this article can be found online at <https://doi.org/10.1016/j.cplett.2023.140327>.

#### References

- [1] A. Paleczek, D. Grochala, K. Staszek, S. Gruszczynski, Erwin Maciak, Zbigniew Opilski, Piotr Kałużyński, Marek Wójcikowski, Tuan-Vu Cao, A. Rydosz, *Sens. Actuata. B: Chem.* 376 (2023) 132964.
- [2] S. Bai, Y. Ma, X. Shu, J. Sun, Y. Feng, R. Luo, D. Li, A. Chen, *Ind. Eng. Chem. Res.* 56 (2017) 2616.
- [3] Y. Wang, Y. Zhou, J. Li, R. Zhang, H. Zhao, Y. Wang, *J. Hazard. Mater.* 435 (2022), 129086.
- [4] J. Li, Y. Zhou, Y. Wang, S. Zhou, R. Zhang, Y. Wang, Z. Zang, *J. Electrochem. Soc.* 169 (2022), 017513.
- [5] Y. Zhou, X. Li, Y. Wang, H.G. Tai, A. Yongcai, *Chem.* 91 (2019) 3311.
- [6] H. Lahlou, S. Claramunt, O. Monereo, D. Prades, J.-M. Fernandez-Sanjuá, N. Bonet, F.-M. Ramos, A. Cirera, *Mater. Today: Proc.* 36 (2021), 19.
- [7] S. Xue, S. Cao, Z. Huang, D. Yang, G. Zhang, *Mater.* 14 (2021) 4263.
- [8] Y. Ren, W. Xie, Y. Li, J. Ma, J. Li, Y. Liu, Y. Zou, Y. Deng, *ACS Cent. Sci.* 11 (2021) 1885.
- [9] M.S. Patil, V.L. Patil, N.L. Tarwal, D.D. More, V.V. Alman, L.D. Kadam, P.S. Patil, J. H. Kim, *J. Electron. Mater.* 48 (2019) 526.
- [10] N. Younes, E.-H. Abd, K.S. Kashyout, M. El-Kemary, *J. Mater. Res. Technol.* 19 (2022) 2633.
- [11] V.V. Ganbavle, J.H. Kim, K.Y. Rajpure, *J. Electron. Mater.* 44 (2015) 874.

- [12] V.V. Ganbavle, S.V. Mohite, J.H. Kim, K.Y. Rajpure, *Curr. Appl. Phys.* 84 (2015) 15.
- [13] G. Adilakshmi, A. Sivasankar Reddy, P. Sreedhara Reddy, Ch. Seshendra Reddy, *Mater. Sci. Eng., B* 273 (2021) 115421.
- [14] S.K. Shaikh, V.V. Ganbavale, S.V. Mohite, U.M. Patil, K.Y. Rajpure, *Superlattices Microstruct.* 120 (2018) 170.
- [15] T. Li, Y. Shen, X. Zhong, S. Zhao, G. Li, B. Cui, D. Wei, K. Wei, J. *Alloys Compd.* 818 (2020), 152927.
- [16] S.B. Karpe, A.D. Bang, D.P. Adhyapak, P.V. Adhyapak, *Sens. Actuat. B: Chem.* 354 (2022), 131203.
- [17] H. Ji, W. Zeng, Y. Li, *Nanoscale* 11 (2019) 22664.
- [18] M. Bonyani, S.M. Zebarjad, K. Janghorban, J.-Y. Kim, H.W. Kim, S.S. Kim, *Chemosensors* 10 (2022) 388.
- [19] T. Wang, A. Chutia, D.J.L. Brett, P.R. Shearing, G. He, G. Chai, I.P. Parkin, *Energy Environ. Sci.* 14 (2021) 2639.
- [20] Q. Li, W. Zeng, Y. Li, *Sens. Actuat. B: Chem.* 359 (2022), 131579.
- [21] V.V. Ganbavle, S.V. Mohite, G.L. Agawane, J. H. Kim and K. Y. Rajpure, *J. Colloid Interface Sci.* 245 (2015) 451.